

Open charm production from d+Au collisions in STAR

M. Calderón de la Barca Sánchez^a on behalf of the STAR Collaboration

J. Adams³, M.M. Aggarwal²⁹, Z. Ahammed⁴³, J. Amonett²⁰, B.D. Anderson²⁰, D. Arkhipkin¹³, G.S. Averichev¹², S.K. Badyal¹⁹, Y. Bai²⁷, J. Balewski¹⁷, O. Barannikova³², L.S. Barnby³, J. Baudot¹⁸, S. Bekele²⁸, V.V. Belaga¹², A. Bellingeri-Laurikainen³⁸, R. Bellwied⁴⁶, J. Berger¹⁴, B.I. Bezverkhny⁴⁸, S. Bharadwaj³³, A. Bhasin¹⁹, A.K. Bhati²⁹, V.S. Bhatia²⁹, H. Bichsel⁴⁵, J. Bielcik⁴⁸, J. Bielcikova⁴⁸, A. Billmeier⁴⁶, L.C. Bland⁴, C.O. Blyth³, S. Blyth²¹, B.E. Bonner³⁴, M. Botje²⁷, A. Boucham³⁸, J. Bouchet³⁸, A.V. Brandin²⁵, A. Bravar⁴, M. Bystersky¹¹, R.V. Cadman¹, X.Z. Cai³⁷, H. Caines⁴⁸, M. Calderón de la Barca Sánchez¹⁷, J. Castillo²¹, O. Catu⁴⁸, D. Cebra⁷, Z. Chajecski²⁸, P. Chaloupka¹¹, S. Chattopadhyay⁴³, H.F. Chen³⁶, Y. Chen⁸, J. Cheng⁴¹, M. Cherney¹⁰, A. Chikanian⁴⁸, W. Christie⁴, J.P. Coffin¹⁸, T.M. Cormier⁴⁶, M.R. Cosentino³⁵, J.G. Cramer⁴⁵, H.J. Crawford⁶, D. Das⁴³, S. Das⁴³, M. Daugherty⁴⁰, M.M. de Moura³⁵, T.G. Dedovich¹², A.A. Derevschikov³¹, L. Didenko⁴, T. Dietel¹⁴, S.M. Dogra¹⁹, W.J. Dong⁸, X. Dong³⁶, J.E. Draper⁷, F. Du⁴⁸, A.K. Dubey¹⁵, V.B. Dunin¹², J.C. Dunlop⁴, M.R. Dutta Mazumdar⁴³, V. Eckardt²³, W.R. Edwards²¹, L.G. Efimov¹², V. Emelianov²⁵, J. Engelage⁶, G. Eppley³⁴, B. Erazmus³⁸, M. Estienne³⁸, P. Fachine⁴, J. Faivre¹⁸, R. Fatemi¹⁷, J. Fedorisin¹², K. Filimonov²¹, P. Filip¹¹, E. Finch⁴⁸, V. Fine⁴, Y. Fisyak⁴, K.S.F. Fornazier³⁵, J. Fu⁴¹, C.A. Gagliardi³⁹, L. Gaillard³, J. Gans⁴⁸, M.S. Ganti⁴³, F. Geurts³⁴, V. Ghazikhanian⁸, P. Ghosh⁴³, J.E. Gonzalez⁸, H. Gos⁴⁴, O. Grachov⁴⁶, O. Grebenyuk²⁷, D. Grosnick⁴², S.M. Guertin⁸, Y. Guo⁴⁶, A. Gupta¹⁹, T.D. Gutierrez⁷, T.J. Hallman⁴, A. Hamed⁴⁶, D. Hardtke²¹, J.W. Harris⁴⁸, M. Heinz², T.W. Henry³⁹, S. Hepplemann³⁰, B. Hippolyte¹⁸, A. Hirsch³², E. Hjort²¹, G.W. Hoffmann⁴⁰, M. Horner²¹, H.Z. Huang⁸, S.L. Huang³⁶, E.W. Hughes⁵, T.J. Humanic²⁸, G. Igo⁸, A. Ishihara⁴⁰, P. Jacobs²¹, W.W. Jacobs¹⁷, M. Jedynek⁴⁴, H. Jiang⁸, P.G. Jones³, E.G. Judd⁶, S. Kabana², K. Kang⁴¹, M. Kaplan⁹, D. Keane²⁰, A. Kechechyan¹², V.Yu. Khodyrev³¹, J. Kiryluk²², A. Kisiel⁴⁴, E.M. Kislov¹², J. Klay²¹, S.R. Klein²¹, D.D. Koetke⁴², T. Kollegger¹⁴, M. Kopytine²⁰, L. Kotchenda²⁵, K.L. Kowalik²¹, M. Kramer²⁶, P. Kravtsov²⁵, V.I. Kravtsov³¹, K. Krueger¹, C. Kuhn¹⁸, A.I. Kulikov¹², A. Kumar²⁹, R.Kh. Kutuev¹³, A.A. Kuznetsov¹², M.A.C. Lamont⁴⁸, J.M. Landgraf⁴, S. Lange¹⁴, F. Laue⁴, J. Lauret⁴, A. Lebedev⁴, R. Lednicky¹², S. Lehocka¹², M.J. LeVine⁴, C. Li³⁶, Q. Li⁴⁶, Y. Li⁴¹, G. Lin⁴⁸, S.J. Lindenbaum²⁶, M.A. Lisa²⁸, F. Liu⁴⁷, H. Liu³⁶, J. Liu³⁴, L. Liu⁴⁷, Q.J. Liu⁴⁵, Z. Liu⁴⁷, T. Ljubicic⁴, W.J. Llope³⁴, H. Long⁸, R.S. Longacre⁴, M. Lopez-Noriega²⁸, W.A. Love⁴, Y. Lu⁴⁷, T. Ludlam⁴, D. Lynn⁴, G.L. Ma³⁷, J.G. Ma⁸, Y.G. Ma³⁷, D. Magestro²⁸, S. Mahajan¹⁹, D.P. Mahapatra¹⁵, R. Majka⁴⁸, L.K. Mangotra¹⁹, R. Manweiler⁴², S. Margetis²⁰, C. Markert²⁰, L. Martin³⁸, J.N. Marx²¹, H.S. Matis²¹, Yu.A. Matulenko³¹, C.J. McClain¹, T.S. McShane¹⁰, F. Meissner²¹, Yu. Melnick³¹, A. Meschanin³¹, M.L. Miller²², N.G. Minaev³¹, C. Mironov²⁰, A. Mischke²⁷, D.K. Mishra¹⁵, J. Mitchell³⁴, B. Mohanty⁴³, L. Molnar³², C.F. Moore⁴⁰, D.A. Mrozov³¹, M.G. Munhoz³⁵, B.K. Nandi⁴³, S.K. Nayak¹⁹, T.K. Nayak⁴³, J.M. Nelson³, P.K. Netrakanti⁴³, V.A. Nikitin¹³, L.V. Nogach³¹, S.B. Nurushev³¹, G. Odyniec²¹, A. Ogawa⁴, V. Okorokov²⁵, M. Oldenborgh²¹, D. Olson²¹, S.K. Pal⁴³, Y. Panebratsev¹², S.Y. Panitkin⁴, A.I. Pavlinov⁴⁶, T. Pawlak⁴⁴, T. Peitzmann²⁷, V. Perevoztchikov⁴, C. Perkins⁶, W. Peryt⁴⁴, V.A. Petrov⁴⁶, S.C. Phatak¹⁵, R. Picha⁷, M. Planinic⁴⁹, J. Pluta⁴⁴, N. Porile³², J. Porter⁴⁵, A.M. Poskanzer²¹, M. Potekhin⁴, E. Potrebenikova¹², B.V.K.S. Potukuchi¹⁹, D. Prindle⁴⁵, C. Pruneau⁴⁶, J. Putschke²¹, G. Rakness³⁰, R. Raniwala³³, S. Raniwala³³, O. Ravel³⁸, R.L. Ray⁴⁰, S.V. Razin¹², D. Reichhold³², J.G. Reid⁴⁵, J. Reinnarth³⁸, G. Renault³⁸, F. Retiere²¹, A. Ridiger²⁵, H.G. Ritter²¹, J.B. Roberts³⁴, O.V. Rogachevskiy¹², J.L. Romero⁷, A. Rose²¹, C. Roy³⁸, L. Ruan³⁶, M.J. Russcher²⁷, R. Sahoo¹⁵, I. Sakrejda²¹, S. Salur⁴⁸, J. Sandweiss⁴⁸, M. Sarsour¹⁷, I. Savin¹³, P.S. Sazhin¹², J. Schambach⁴⁰, R.P. Scharenberg³², N. Schmitz²³, K. Schweda²¹, J. Seger¹⁰, P. Seyboth²³, E. Shahaliev¹², M. Shao³⁶, W. Shao⁵, M. Sharma²⁹, W.Q. Shen³⁷, K.E. Shestermanov³¹, S.S. Shimanskiy¹², E. Sichtermann²¹, F. Simon²³, R.N. Singaraju⁴³, N. Smirnov⁴⁸, R. Snellings²⁷, G. Sood⁴², P. Sorensen²¹, J. Sowinski¹⁷, J. Speltz¹⁸, H.M. Spinka¹, B. Srivastava³², A. Stadnik¹², T.D.S. Stanislaus⁴², R. Stock¹⁴, A. Stolpovsky⁴⁶, M. Strikhanov²⁵, B. Stringfellow³², A.A.P. Suaide³⁵, E. Sugarbaker²⁸, C. Suire⁴, M. Sumner¹¹, B. Surrow²², M. Swanger¹⁰, T.J.M. Symons²¹, A. Szanto de Toledo³⁵, A. Tai⁸, J. Takahashi³⁵, A.H. Tang²⁷, T. Tarnowsky³², D. Thein⁸, J.H. Thomas²¹, S. Timoshenko²⁵, M. Tokarev¹², T.A. Trainor⁴⁵, S. Trentalange⁸, R.E. Tribble³⁹, O.D. Tsai⁸, J. Ulery³², T. Ullrich⁴, D.G. Underwood¹, G. Van Buren⁴, M. van Leeuwen²¹, A.M. Vander Molen²⁴, R. Varma¹⁶, I.M. Vasilevski¹³, A.N. Vasiliev³¹, R. Vernet¹⁸, S.E. Vigdor¹⁷, Y.P. Viyogi⁴³, S. Vokal¹², S.A. Voloshin⁴⁶, W.T. Waggoner¹⁰, F. Wang³², G. Wang²⁰, G. Wang⁵, X.L. Wang³⁶, Y. Wang⁴⁰, Y. Wang⁴¹, Z.M. Wang³⁶, H. Ward⁴⁰, J.W. Watson²⁰, J.C. Webb¹⁷, G.D. Westfall²⁴, A. Wetzler²¹, C. Whitten Jr.⁸, H. Wieman²¹, S.W. Wissink¹⁷, R. Witt², J. Wood⁸, J. Wu³⁶, N. Xu²¹, Z. Xu⁴,

^a e-mail: mc@bnl.gov

Z.Z. Xu³⁶, E. Yamamoto²¹, P. Yepes³⁴, V.I. Yurevich¹², I. Zborovsky¹¹, H. Zhang⁴, W.M. Zhang²⁰, Y. Zhang³⁶, Z.P. Zhang³⁶, R. Zoukarneev¹³, Y. Zoukarneeva¹³, A.N. Zubarev¹²

- ¹ Argonne National Laboratory, Argonne, Illinois 60439, USA
- ² University of Bern, 3012 Bern, Switzerland
- ³ University of Birmingham, Birmingham, UK
- ⁴ Brookhaven National Laboratory, Upton, New York 11973, USA
- ⁵ California Institute of Technology, Pasadena, California 91125, USA
- ⁶ University of California, Berkeley, California 94720, USA
- ⁷ University of California, Davis, California 95616, USA
- ⁸ University of California, Los Angeles, California 90095, USA
- ⁹ Carnegie Mellon University, Pittsburgh, Pennsylvania 15213, USA
- ¹⁰ Creighton University, Omaha, Nebraska 68178, USA
- ¹¹ Nuclear Physics Institute AS CR, 250 68 Řež/Prague, Czech Republic
- ¹² Laboratory for High Energy (JINR), Dubna, Russia
- ¹³ Particle Physics Laboratory (JINR), Dubna, Russia
- ¹⁴ University of Frankfurt, Frankfurt, Germany
- ¹⁵ Institute of Physics, Bhubaneswar 751005, India
- ¹⁶ Indian Institute of Technology, Mumbai, India
- ¹⁷ Indiana University, Bloomington, Indiana 47408, USA
- ¹⁸ Institut de Recherches Subatomiques, Strasbourg, France
- ¹⁹ University of Jammu, Jammu 180001, India
- ²⁰ Kent State University, Kent, Ohio 44242, USA
- ²¹ Lawrence Berkeley National Laboratory, Berkeley, California 94720, USA
- ²² Massachusetts Institute of Technology, Cambridge, MA 02139-4307, USA
- ²³ Max-Planck-Institut für Physik, Munich, Germany
- ²⁴ Michigan State University, East Lansing, Michigan 48824, USA
- ²⁵ Moscow Engineering Physics Institute, Moscow Russia
- ²⁶ City College of New York, New York City, New York 10031, USA
- ²⁷ NIKHEF and Utrecht University, Amsterdam, The Netherlands
- ²⁸ Ohio State University, Columbus, Ohio 43210, USA
- ²⁹ Panjab University, Chandigarh 160014, India
- ³⁰ Pennsylvania State University, University Park, Pennsylvania 16802, USA
- ³¹ Institute of High Energy Physics, Protvino, Russia
- ³² Purdue University, West Lafayette, Indiana 47907, USA
- ³³ University of Rajasthan, Jaipur 302004, India
- ³⁴ Rice University, Houston, Texas 77251, USA
- ³⁵ Universidade de Sao Paulo, Sao Paulo, Brazil
- ³⁶ University of Science & Technology of China, Anhui 230027, China
- ³⁷ Shanghai Institute of Applied Physics, Shanghai 201800, China
- ³⁸ SUBATECH, Nantes, France
- ³⁹ Texas A&M University, College Station, Texas 77843, USA
- ⁴⁰ University of Texas, Austin, Texas 78712, USA
- ⁴¹ Tsinghua University, Beijing 100084, China
- ⁴² Valparaiso University, Valparaiso, Indiana 46383, USA
- ⁴³ Variable Energy Cyclotron Centre, Kolkata 700064, India
- ⁴⁴ Warsaw University of Technology, Warsaw, Poland
- ⁴⁵ University of Washington, Seattle, Washington 98195, USA
- ⁴⁶ Wayne State University, Detroit, Michigan 48201, USA
- ⁴⁷ Institute of Particle Physics, CCNU (HZNU), Wuhan 430079, China
- ⁴⁸ Yale University, New Haven, Connecticut 06520, USA
- ⁴⁹ University of Zagreb, Zagreb, 10002, Croatia

Received: 9 April 2005 / Revised version: 15 April 2005 /

Published online: 2 August 2005 – © Springer-Verlag / Società Italiana di Fisica 2005

Abstract. Charmed hadrons are interesting observables in heavy ion collisions. They are becoming more accessible to experimental scrutiny at RHIC energies due to the increased production cross-section of charm with the larger centre-of-mass energy available at RHIC compared to SPS. One source of interest in charm production is due to the fact that gluon fusion dominates the charm production cross-section at high energy. Hence, a measurement of charm hadrons is directly sensitive to the gluon distributions of the colliding particles. In addition, any measurement of J/ψ production at RHIC, and more importantly

any observed suppression, must be compared to the overall production of $c\bar{c}$ pairs. A systematic study of charmed hadrons in all collision systems available at RHIC is therefore an invaluable experimental tool in the characterization of the matter produced at RHIC. In particular, d+Au collisions are a necessary step for the comparison of any possible modification of charm production in Au+Au collisions. We present preliminary results on D meson production from d+Au collisions in STAR at $\sqrt{s_{NN}} = 200$ GeV.

PACS. 13.20.Fc, 13.25.Ft, 25.75.-q, 24.85.+p

1 Introduction

Heavy flavour hadrons are of interest to study in heavy ion collisions for several reasons. Due to the large mass of the charm quark, it is possible to treat charm production in perturbative calculations (see e.g. [1]). The total charm yield is expected to be less sensitive to soft processes, making charm observables a robust standard in hadronic collisions to study QCD. For example, the suppression of the charmonium states in central collisions at SPS energies, and its interpretation have been the subject of detailed scrutiny. The typical measurement involves measuring the J/ψ cross section in a given system and taking a ratio with respect to Drell-Yan production in the same system [2]. At RHIC energies, in order to normalize the charmonium production, it will be necessary to measure not Drell-Yan but the charm production cross section, $\sigma_{c\bar{c}}$.

More recent theoretical questions have to do with the production of heavy flavour *per se*. An enhancement of charm via preequilibrium parton collisions has been suggested as a probe of the thermalization time [3]. If a deconfined region is formed at RHIC which still might have a significant amount of interactions among the partonic constituents (light quarks and gluons), it is possible that heavy quarks produced in an initial hard scattering could thermalize with the evolving medium. It would be hard to imagine that charm quarks could thermalize if deconfinement is not reached. Recently, a mechanism for speeding up the thermalization of charm quarks in a QGP has been proposed. Above the critical temperature ($T_c \simeq 170$ MeV, hadron-like states might still survive [4–7]). The charm quarks produced mainly in the first collisions might then rescatter through these hadron-like resonances, where the charm cross section for the scattering with these states is expected to be larger than for normal hadrons. This effect would lead to a rapid thermalization of charm quarks above T_c , modifying significantly their original kinematics. Therefore, not only the production cross-section but the spectra of charmed hadrons have become of renewed importance. A measurement of a large elliptic flow amplitude for charm quarks would in this context also be a powerful indicator for significant in-medium interactions. Preliminary results indicate that the elliptic flow of charm quarks is as strong as it is for light quarks [8,9]. It would be extremely unlikely to develop a strong elliptic flow in the charm sector via only hadronic interactions, so this would be evidence that the anisotropy is developed at the partonic level.

A program of studying heavy flavour production is therefore a crucial component of the characterization of the matter produced at RHIC. A measurement of $\sigma_{c\bar{c}}$ and

of the transverse momentum distribution of open-charm in pp, d + Au and Au + Au collisions is one of the first tasks. In this paper, we present progress on the analysis of open charm production in d + Au collisions.

2 Data analysis

The results presented here come from data taken during the 2003 run at RHIC with the Solenoidal Tracker at RHIC (STAR) experiment [10]. The measurements were done with d + Au beams at $\sqrt{s_{NN}} = 200$ GeV. We used a total of 15.7 million minimum bias d + Au events for the offline analysis.

The main detector component used in this study was the Time Projection Chamber (TPC). The details of the detector can be found elsewhere (e.g. [11]). The TPC track reconstruction provides information on the momenta of the particles and, together with measurements of the ionization energy loss (dE/dx), identification of π and K mesons up to ~ 700 MeV/c. We reconstructed the open charm mesons through the decays $D^0 \rightarrow K^- + \pi^+$ (B.R. 3.8%) and $D^{*+}(2010) \rightarrow D^0 + \pi^+$ (B.R. 68%) [12] with a subsequent decay of the D^0 in the $K^-\pi^+$ channel, so the combined B.R. = 2.6%. The charge-conjugate decays are implied in all cases throughout this paper.

The pointing accuracy obtained from the TPC is not sufficient to distinguish displaced vertices of the D meson decays ($c\tau(D^0) = 123 \mu\text{m}$) [12], so the analysis was implemented using all possible combinations of track candidates in the same event. For a background estimation, a similar combination was done taking tracks from mixed events. For the case of the D^0 , the signal to background ratio obtained with this method was found to be $S/B = 1/600$.

For the analysis of D^0 , we used tracks within $|\eta| < 1$ where η is the pseudorapidity. We also required the transverse momentum, p_T , of a track to be in the range $0.2 < p_T < 10$ GeV/c, and the total momentum to be in the range $0.3 < p < 10$ GeV/c.

The invariant mass spectrum after subtraction of the mixed event background was found to be well reproduced by a gaussian plus a linear background. Simulation studies reproduced the features of the residual linear background. We attribute the residual background to correlations present in the same events such as di-hadron correlations from jet fragmentation which are not present in the mixed event sample. The invariant mass spectrum for the $D^0 \rightarrow K + \pi$ analysis after subtraction of the mixed-event background is shown in Fig. 1, top panel. The reconstructed invariant mass from the fit is 1.863 ± 0.003 GeV/ c^2 , consistent with the PDG value of $1.8646 \pm$

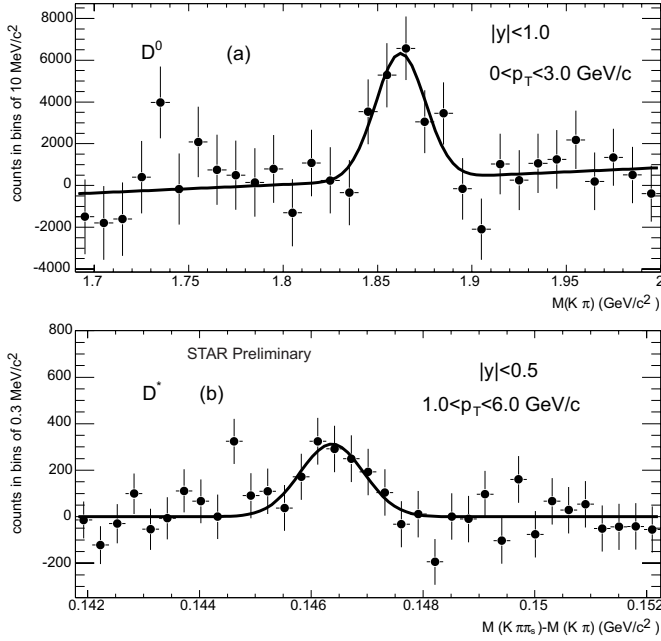


Fig. 1. The invariant mass distribution of the $K + \pi$ system (top panel) and of the $K + \pi + \pi_s - K + \pi$ combination (bottom panel), where π_s is the lowest momentum (i.e. “soft”) pion in the decay

$0.0005 \text{ GeV}/c^2$ [12]. The width is $13.8 \pm 2.8 \text{ MeV}/c^2$ which is consistent with that expected from the momentum resolution obtained from detector simulations.

For the analysis of D^{*+} , we took specialized runs with a magnetic field strength of $B = 0.25 \text{ T}$, half the nominal value used in STAR. This was done to increase the detector acceptance for the second pion in the decay, which is typically very soft. The typical momentum of the soft pion is $\sim 50 \text{ MeV}/c$ which is not enough for it to produce a track with sufficient points (~ 20 or more) for accurate reconstruction with a magnetic field of $B = 0.5 \text{ T}$.

The track selection criteria for the D^{*+} were as follows. Tracks were accepted in the range $|\eta| < 1.5$. For the reconstruction of the kaon and pion from the D^0 decay, the momenta of the tracks used were restricted to the range $0.3 < p < 10 \text{ GeV}/c$. The momentum of the soft pion (π_s) was restricted to the range $0.1 < p < 1.0 \text{ GeV}/c$ in order to ensure good reconstruction efficiency in the full momentum range (the efficiency drops rapidly below this cutoff). The ratio of the reconstructed D^0 momentum to that of the soft pion was also restricted to be $p(D^0)/p(\pi_s) > 9.0$. The D^{*+} reconstruction was done as follows. First, a kaon and pion were used to find candidate D^0 mesons by restricting them to have an invariant mass in the range $1.82 < M(K\pi) < 1.90 \text{ GeV}/c^2$. We then combined these with a soft pion candidate which was also required to have an opposite charge sign to that of the kaon. This produced a D^{*+} candidate having invariant mass $M(K\pi\pi_s)$. The bottom panel of Fig. 1 shows the distribution of the mass difference $M(K\pi\pi_s) - M(K\pi)$ for the D^{*+} candidates after all cuts and a mixed event background subtraction. The fit to the mass difference spectrum us-

ing a gaussian gives a mean of $146.37 \pm 0.12 \text{ MeV}/c^2$. This is larger than the PDG value of $m_{D^{*+}} - m_{D^0} = 145.421 \pm 0.010 \text{ MeV}/c^2$ due to our imposed momentum cutoff on π_s of $p > 100 \text{ MeV}/c$.

To correct the yields, a standard embedding analysis was performed. This consisted of simulated open charm mesons inserted into real data events. The decay daughters are passed through the simulator of the detector response and combined with a real event at the level of the raw data. In this form, they can be processed through the same reconstruction and analysis software. We find that the reconstruction efficiency for D^0 is in the range 40–60% (increasing with p_T). The efficiency for D^{*+} reconstruction is much smaller than would be expected from another 3-body decay because of the lower reconstruction efficiency of the soft pion (e.g. it is 6% at the lowest measured D^{*+} p_T).

3 Results and discussion

Figure 2 shows the invariant K yield of D^0 and D^{*+} as a function of transverse momentum, after correcting the raw yield of D^0 and D^{*+} for the reconstruction efficiency, acceptance, trigger efficiency and event vertex-finding efficiency.

For the D^0 analysis, there was an additional correction from a Monte Carlo study of the correlations introduced by the misidentification of the kaon and pion. Statistical errors are shown. The analysis measures both particles and anti-particles, so the data are scaled down by a factor of 2. This is done so that we can use the numbers from the fit to the spectra to obtain the yield and then estimate from it the $c\bar{c}$ cross section as described below. The D^{*+} data are scaled by the ratio D^{*+}/D^0 which is obtained in the following way. We fit the p_T spectrum of both the D^0

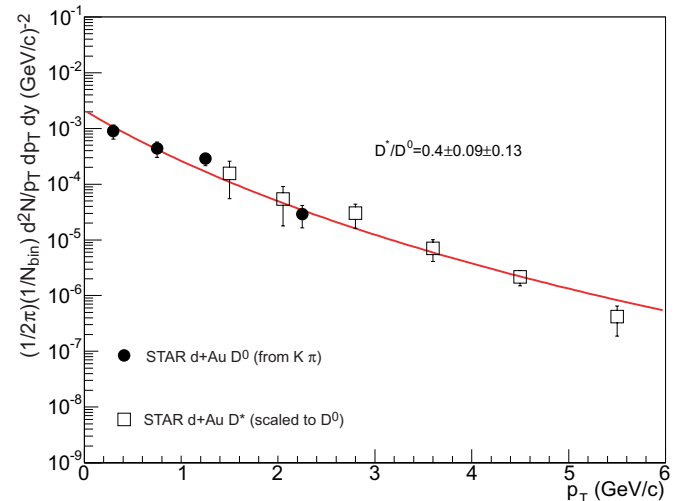


Fig. 2. The combined transverse momentum (p_T) spectra of D^0 (filled circles) and D^{*+} (open squares) from minimum bias d + Au collisions. The D^{*+} yields are scaled to the D^0 (see text). The line is a power-law fit to the combined p_T spectrum

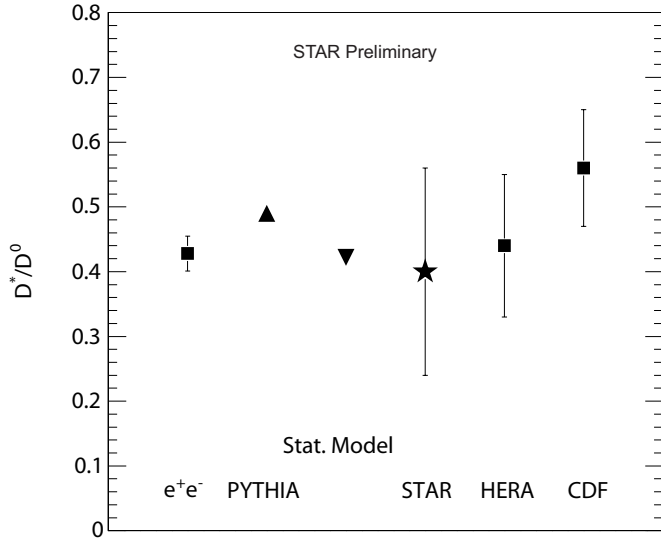


Fig. 3. The ratio of the yield of D^{*+} to D^0 mesons. Comparisons to results from e^+e^- , $e+p$ and $p+\bar{p}$ collisions and from PYTHIA [15] calculations are also shown

and D^{*+} to a power law with the form $A(1 + p_T/p_0)^{-n}$ with an additional free parameter for the D^{*+}/D^0 ratio.

We obtain a value of $D^{*+}/D^0 = 0.40 \pm 0.09_{\text{stat}} \pm 0.13_{\text{syst}}$. Within the large uncertainties, this is consistent with the measured ratios from e^+e^- , HERA [13], and CDF at the Tevatron [14]. This is shown in Fig. 3. For example, from the fragmentation fractions measured at HERA [13] we find $f(c \rightarrow D^0) = 0.66 \pm 0.05^{+0.12}_{-0.14} +0.09_{-0.05}$ and $f(c \rightarrow D^{*+}) = 0.26 \pm 0.02^{+0.06}_{-0.04} +0.03_{-0.02}$, where the first uncertainty is statistical, the second is systematic and the third is from theory. Taking the ratio and taking into account only the statistical error (which is probably a good assumption, since the theoretical uncertainty should cancel, as well as some of the systematics) would give $D^{*+}/D^0 = 0.39 \pm 0.05$.

Figure 2 shows the D^{*+} data scaled by the ratio obtained in this manner, and the line is the power-law fit used in the procedure. From the fit, we obtain an invariant yield per unit of rapidity at $y = 0$ of $dN/dy(D^0) = 0.0265 \pm 0.0036_{\text{stat}} \pm 0.0071_{\text{syst}}$. The mean transverse momentum of the open charm mesons is also found from the fit: $\langle p_T \rangle = 1.32 \pm 0.08_{\text{stat}} \pm 0.16_{\text{syst}}$ GeV/c. We can estimate the charm cross section $\sigma_{c\bar{c}}$ by the following procedure. We assume that the ratio $D^+/D^0 \approx D^{*+}/D^0$. This assumption is consistent with the world average e^+e^- data. The fragmentation fraction of D^{*+} in e^+e^- collisions is $f(c \rightarrow D^{*+}) = 0.24 \pm 0.01$ and the one for D^+ is $f(c \rightarrow D^+) = 0.23 \pm 0.02$ [13]. This gives a ratio of $D^{*+}/D^+ = 1.0 \pm 0.1$. (In other systems, this assumption is slightly less justified: from the fragmentation fractions measured at HERA in the same [13], the corresponding ratio is $D^{*+}/D^+ = 1.3 \pm 0.2$, so the assumption carries an additional systematic uncertainty of about 20%). This provides an estimate for the yield of D^+ , which can then be used to estimate $\sigma_{c\bar{c}} = 1.24(\sigma(D^0) + \sigma(D^{*+}))$ where the factor 1.24 is used to take into account contributions from D_s and charmed baryons (Λ_c , etc.). In [16], this is

used in DIS; we assume that it can also be applied here. The D^0 cross section is estimated from the invariant yield applying the following factors. To scale from dN/dy at $y = 0$ to full phase space, we use a PYTHIA calculation [17] and obtain a factor of 4.7 ± 0.7 . We assume that the charm yield in d + Au scales with the number of binary collisions, N_{bin} . The mean number of binary collisions for minimum bias d + Au collisions is estimated from a Glauber model calculation: $\langle N_{\text{bin}} \rangle = 7.5 \pm 0.4$ [18]. Finally, we use the pp non single-diffractive minimum bias cross section $\sigma_{pp} = 42$ mb. We estimate the D^0 cross section as $\sigma_{D^0} = 4.7 \times (dn/dy) \times \sigma_{pp} / \langle N_{\text{bin}} \rangle$. To get the estimate for $\sigma_{c\bar{c}}$, we multiply this by 1.4×1.24 as discussed above to take into account the D^+ and contributions from D_s and Λ_c , obtaining $\sigma_{c\bar{c}} = 1.2 \pm 0.2_{\text{stat}} \pm 0.4_{\text{syst}}$ mb. This is consistent with the results using the low p_T D^0 data only [20]. This is almost a factor of 2 larger than the one quoted by PHENIX [19]. However, the PHENIX measurement is done in pp collisions. If there is an enhancement of the yield of D mesons in d + Au collisions (e.g. due to the Cronin effect), the strict binary collision scaling will not hold. A Cronin-like enhancement in d + Au collisions would then lead to an apparent increase in the cross section if one applies binary collision scaling. The current data from STAR on the non-photonic electron nuclear modification factor [21] are consistent with no enhancement within errors, but can also allow for enhancements of 30 or 40%, so more precise measurements of this would be useful. Nevertheless, the discrepancy between this estimate and the PHENIX measurement based on their electron spectrum is a 1.6 standard-deviation effect.

As a way to check the consistency of the STAR results, we compared the open charm meson reconstruction data to the single electron spectrum. There were two analyses done to measure the spectrum at low p_T . One analysis was performed doing a combined identification using a small acceptance Time-of-Flight prototype (TOF) together with TPC information (momentum and dE/dx) [20]. The small azimuthal acceptance ($\Delta\phi = 0.1$) limited the reach to $p_T = 3$ GeV/c. A separate analysis using only dE/dx information was also performed to profit from the large TPC acceptance, allowing statistics to reach $p_T = 4$ GeV/c. For high p_T , the STAR Barrel Electromagnetic Calorimeter was also used to identify electrons. The high p_T electron analysis is discussed in [21]. The directly measured single electron spectrum was corrected for photonic sources. These are mainly produced by photon conversions in the detector material and by π^0 Dalitz decays. By reconstructing the invariant mass and opening angle distributions of e^+e^- pairs, together with estimates for the reconstruction efficiency of these sources estimated from simulation ($\sim 60\%$ efficiency for electrons with $p_T > 1$ GeV/c), it is possible to measure the contribution from these photonic sources and subtract them from the directly measured electrons. Contributions from the semi-leptonic decays of η , ω , ρ , ϕ and K mesons were estimated from simulations.

The resulting “non-photonic” electron spectrum is expected to be dominated by the semi-leptonic decay of heavy quarks. From the open charm p_T spectrum, we

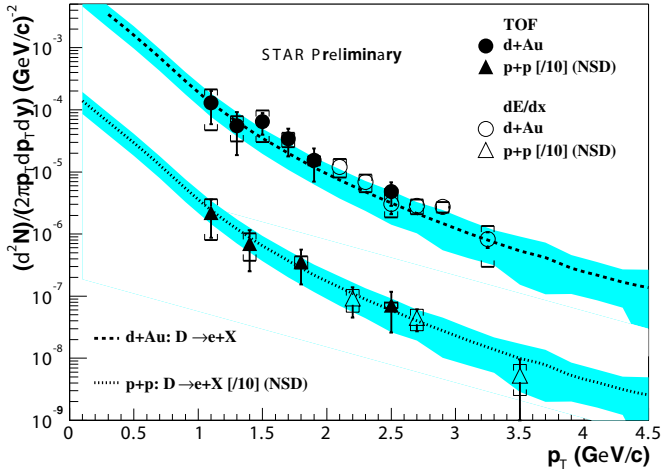


Fig. 4. The single electron p_T spectrum measured by STAR. The lines represent the signal expected from the semi-leptonic decay of charm inferred from a fit to the measured p_T spectrum of D mesons (Fig. 2), the shaded band is the systematic uncertainty

can estimate the contribution to the electron spectrum from semi-leptonic charm decays. Figure 4 shows the background subtracted non-photonic electron spectrum measured in d + Au (circles) and pp (triangles) collisions. The pp data measured in STAR corresponds to the non single-diffractive (NSD) part of the pp cross section. The filled symbols are from the combined analysis of TOF + TPC data; open symbols are from TPC only data.

The dashed lines on the figure are the spectra obtained from the open charm meson p_T spectra by generating semi-leptonic decays. This is done in the following way. We take as input the p_T distribution of the D mesons. We assume that within our acceptance ($|y| < 1$), the rapidity distribution is flat. We then simulate D meson decays in which there is an electron in the final state (e.g. $D^0 \rightarrow K^- e^+ \nu_e$ with B.R. 3.58%, $D^0 \rightarrow K^- \pi^0 e^+ \nu_e$ with B.R. 1.1%, etc.). We use 4 such semi-leptonic decay chains for D^0 and 2 for the D^+ . This will produce an electron spectrum from the decay of charm mesons which we use to compare to the measured non-photonic electron spectrum. The shaded region shows the systematic uncertainty in the shape of the electron spectra derived from the open charm data. The line for the pp data is the same as the one for the d + Au data but scaled down by $\langle N_{\text{bin}} \rangle = 7.5$. Within the uncertainties, the electron data up to $p_T \simeq 4$ GeV/c can be described well by the contributions from charm decays.

4 Conclusions and outlook

We have presented measurements of D^0 and D^{*+} production in d + Au collisions at RHIC. The identification of pions and kaons in the TPC allows for a reconstruction of open charm mesons. We are currently studying the feasibility of reconstructing additional decay modes. The D^0 and D^{*+} p_T spectrum can be fit to a power-law shape,

from which we obtain $D^{*+}/D^0 \simeq 0.4$. The yield of D^0 can also be used to obtain an estimate for the charm cross section under the assumption that binary collision scaling holds. We estimate $\sigma_{c\bar{c}} \simeq 1.18$ mb. On one hand, this is larger than the PHENIX measurement by about a factor of 2; on the other hand, the difference is only significant to 1.6σ . To resolve these discrepancies, reconstruction of the non-photonic electron spectrum at $\sqrt{s_{\text{NN}}}=200$ GeV from both STAR and PHENIX would be useful to remove ambiguities related to the obtention of the electron spectrum from that of open charm. In addition, reconstruction of open charm mesons in pp in order to test the assumption of the scaling with binary collisions is desirable. The large value of the charm cross section is also very difficult to reconcile with NLO pQCD calculations [22]. The experimental effects which might cause such discrepancies are being actively investigated.

References

1. M.L. Mangano et al., Nuc. Phys. B **405**, 507 (1993)
2. B. Alessandro et al. [NA50 Collaboration], Eur. Phys. J. C **39**, 335 (2005) [arXiv:hep-ex/0412036]
3. B. Muller, X.N. Wang, Phys. Rev. Lett. **68**, 2437 (1992)
4. E.V. Shuryak, I. Zahed, Phys. Rev. C **70**, 021901 (2004) [arXiv:hep-ph/0307267]
5. G. E. Brown, C.H. Lee, M. Rho, E. Shuryak, Nucl. Phys. A **740**, 171 (2004) [arXiv:hep-ph/0312175]
6. X. Li, H. Li, C. M. Shakin, Q. Sun, Phys. Rev. C **69**, 065201 (2004) [arXiv:hep-ph/0403066]
7. H. van Hees, R. Rapp, arXiv:nucl-th/0412015
8. M. Kaneta et al., [PHENIX Collaboration], J. Phys. G **30**, S1217 (2004) [arXiv:nucl-ex/0404014]
9. F. Laue et al., [STAR Collaboration], arXiv:nucl-ex/0411007
10. K.H. Ackermann et al. [STAR Collaboration], Nucl. Instrum. Meth. A **499**, 624 (2003)
11. M. Anderson et al., Nucl. Instrum. Meth. A **499**, 659 (2003) [arXiv:nucl-ex/0301015]
12. S. Eidelman et al. [Particle Data Group], Phys. Lett. B **592** (2004) 1
13. U. Karshon et al., [H1 Collaboration], Nucl. Phys. Proc. Suppl. **126**, 179 (2004) [arXiv:hep-ex/0307007]
14. D. Acosta et al. [CDF Collaboration], Phys. Rev. Lett. **91**, 241804 (2003) [arXiv:hep-ex/0307080]
15. T. Sjostrand, P. Eden, C. Friberg, L. Lonnblad, G. Miu, S. Mrenna, E. Norrbin, Comput. Phys. Commun. **135**, 238 (2001) [arXiv:hep-ph/0010017]
16. B. A. Kniehl, F. Sefkow, arXiv:hep-ph/0312054
17. Modified parameters are: MSEL=1 (minbias events), CTEQ5M1 PDF, $\langle k_t \rangle = 2$ GeV/c, $m_c = 1.7$ GeV/c², $K = 2.2$, MSTP(32)=4 (Q^2) and PARP(67)=4 (factor multiplied to Q^2)
18. J. Adams et al. [STAR Collaboration], Phys. Rev. Lett. **91**, 072304 (2003) [arXiv:nucl-ex/0306024]
19. S. Kelly et al., [PHENIX Collaboration], J. Phys. G **30**, S1189 (2004) [arXiv:nucl-ex/0403057]
20. J. Adams et al. [STAR Collaboration], Phys. Rev. Lett. **94**, 062301 (2005) [arXiv:nucl-ex/0407006]
21. A. Suaide et al., [STAR Collaboration], these proceedings
22. R. Vogt [Hard Probe Collaboration], Int. J. Mod. Phys. E **12**, 211 (2003) [arXiv:hep-ph/0111271]